MODEL PREDICTIONS AND EXPERIMENTAL RESULTS FOR THE ROTORDYNAMIC CHARACTERISTICS OF LEAKAGE FLOWS IN CENTRIFUGAL PUMPS

by

Adiel Guinzburg

Research Scientist

Institut de Machines Hydraulics et de Mécanique des Fluides

Ecole Polytechnique Fédérale

Lausanne, Switzerland

and

Christopher E. Brennen

Professor, Mechanical Engineering, Dean of Students

California Institute of Technology

Pasadena, California

Adiel Guinzburg is a Research Scientist at the Institut de Machines Hydrauliques et de Mécanique des Fluides at the Ecole Polytechnique Fédérale de Lausanne, Switzerland. She holds a B.Sc. degree in Aeronautical Engineering from the University of the Witwatersrand and M.S. and Ph.D. degrees from the California Institute of Technology.

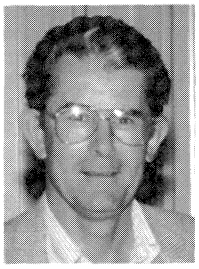

Christopher E. Brennen is a Professor of Mechanical Engineering and Dean of Students at the California Institute of Technology in Pasadena, California. He holds B.A., M.A., and D.Phil. degrees in Engineering Science from Oxford University. He has been honored by ASME. He has won the ASME Knapp Award twice and is this year's recipient of the ASME Fluids Engineering Award. He is a consultant and has over 120 technical publications.

ABSTRACT

The role played by fluid forces in determining the rotordynamic stability and characteristics of a centrifugal pump is gaining increasing attention. The present research investigates the contributions to the rotordynamic forces from the discharge-to-suction leakage flows between the front shroud of the rotating impeller and the stationary pump casing. An experiment was designed to measure the rotordynamic shroud forces due to simulated leakage flows for different parameters such as flowrate, shroud clearance, face seal clearance, and eccentricity. The functional dependence on the ratio of whirl frequency to rotating frequency (termed the whirl ratio) is very similar to that measured in experiments and similar to that predicted by the theoretical work of Childs [1]. Childs' bulk flow model yielded some unusual results including peaks in the rotordynamic forces at particular positive whirl ratios, a phenomenon which Childs tentatively described as a "resonance" of the leakage flow. This unexpected phenomenon developed at small positive whirl ratios when the inlet swirl velocity ratio exceeds about 0.5. Childs points out that a typical swirl velocity ratio at inlet (pump discharge) would be about 0.5 and may not, therefore, be large enough for the resonance to be manifest. To explore whether this effect occurs, an inlet guide vane was constructed which introduced a known amount of swirl into the flow upstream of the leakage flow inlet. A detailed comparison of model predictions with the present experimental program is presented. The experimental results showed no evidence of the "resonances," even at much larger swirl inlet velocities than explored by Childs.

INTRODUCTION

The interaction of a centrifugal pump impeller and the working fluid can cause various forces on the rotor. Some of these may cause self-excited whirl in which the axis of rotation of the impeller moves along a trajectory eccentric to the undeflected position. It is important to be able to predict these fluid-induced forces during the design phase. There is an ongoing effort dealing with an improvement in predicting the rotordynamic behavior of pumps (Frei, et al. [2], Pace, et al. [3], and Verhoeven [4]). This study has focused attention on one source of such whirl excitation, namely the forces acting on the shroud of an impeller due to the discharge-to-suction leakage flows external to the impeller.

Rotordynamic forces imposed on a centrifugal pump by the fluid flow were first measured by Domm and Hergt [5], Hergt and Krieger [6], Chamieh, et al. [7], and Jery, et al. [8]. In the Rotor Force Test Facility (RFTF) at Caltech (Jery, et al., [8]; Adkins, et al., [9]; Franz, et al., [10]) known whirl motions over a full range of frequencies (subsynchronous, supersynchronous, and reverse whirl) are superimposed on the normal motion of an impeller. This facility was also used for the present experiments. Fluid forces on a rotating centrifugal impeller in a whirling motion have also been measured at the University of Tokyo, by Ohashi and Shoji [11]. Bolleter, et al. [12], also made an experimental determination of the hydrodynamic force matrices. It can be seen that there is an international attempt to understand these forces.

The hydrodynamic force on a rotating shroud or impeller (Figure 1) which is whirling can be expressed in the stationary laboratory frame in linear form as:

$$\begin{bmatrix} F^*_x(t) \\ F^*_y(t) \end{bmatrix} = \begin{bmatrix} F^*_{ox} \\ F^*_{oy} \end{bmatrix} + [A^*] \begin{bmatrix} x^*(t) \\ y^*(t) \end{bmatrix} \qquad (1)$$

Here, F^*_{ox}, F^*_{oy}, are the steady radial forces in the absence of whirl motion and are discussed in detail elsewhere (Iversen, et al. [13], Domm and Hergt [5], Chamieh [14], Chamieh, et al. [7],

Adkins [15]). The matrix [A*] is the rotordynamic matrix which will, in general, be a function not only of the mean flow conditions and pump geometry but also of the frequency of whirl, Ω. If outside the linear range, it may also be a function of the amplitude of the whirl motion, ε. At small, linear amplitudes, [A*] should be independent of ε, and can be presented as a function of the whirl ratio Ω/ω where ω is the impeller rotation frequency. In the case of the circular whirl orbits used in the present experiments, $x^* = \varepsilon \cos \Omega t$, $y^* = \varepsilon \sin \Omega t$. The reader is referred to Jery, et al. [8] and Franz, et al. [10], for further details.

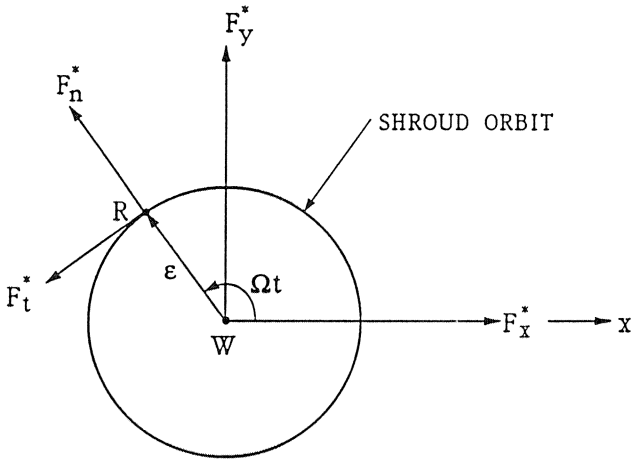

Figure 1. Schematic Representation of the Fluid-Induced Radial Forces Acting on an Impeller Whirling in a Circular Orbit. F_x^* and F_y^* represent the instantaneous forces in the stationary laboratory frame. F_n^* and F_t^* are the forces normal and tangential to the whirl orbit where Ω is the whirl frequency.

Herein, the preceding equations will be expressed in nondimensional terms. The unsteady forces normal and tangential to the imposed circular whirl orbit, F_n^* and F_t^*, are nondimensionalized by $\rho\pi\omega\ {}^2R_2{}^3b_2/R_2$. This method is typical (e.g., Ohashi and Shoji [11], Bolleter, et al. [12]). If [A] is to be rotationally invariant, then

$$\begin{aligned} Fn &= A_{xx} = A_{yy} \\ Ft &= A_{xy} = -A_{yx} \end{aligned} \tag{2}$$

The experimental observations of Jery, et al. [8] and Adkins, et al. [9], on centrifugal pump impellers demonstrated that there are two sources for these fluid-induced forces. It was recognized that contributions to the rotordynamic forces could arise from azimuthally nonuniform pressures in the discharge flow acting on the impeller discharge area and from similar nonuniform pressures acting on the exterior of the impeller front shroud, as a result of the leakage flow passing between this shroud and the pump casing.

Adkins, et al. [9], demonstrated both analytically and experimentally that the leakage flow from the discharge through the gap outside the impeller shroud to the inlet was responsible for significant nonuniformity in the pressure acting on the exterior of the shroud and that this contributed to both the radial forces and rotordynamic matrices. Parallel to the experimental investigation, a fluid mechanical model of the complicated unsteady throughflow generated when a rotating impeller whirl was developed by Adkins [15]. It is quasi- one-dimensional and requires only the geometry of the impeller and volute and the impeller/volute performance curve. The model allowed evaluation of the pressure perturbations in the impeller discharge which compared well with the experimental measurements of these perturbations. Tsujimoto, et al. [16], examined the two or three dimensional character of the unsteady flow in order to establish the complex relationship between the vorticity shed by the impeller blades and the forces on the impeller.

There are several other indications which suggest the importance of leakage flows to the fluid-induced rotordynamic forces. It is striking that the total rotordynamic forces measured by Bolleter, et al. [12], for a conventional centrifugal pump configuration are about twice the magnitude of those measured by Jery [17] or Adkins [15]. Both test programs used a radial face seal to minimize the forces which would be developed by the wear-ring seals. So the measured hydrodynamic forces are due to a combination of the impeller-volute and the impeller-shroud interaction. It now seems sensible to suggest that this difference is due to the fact that the clearance in Bolleter's leakage flow annulus is substantially smaller than in the experiments of Jery and Adkins.

When it became apparent that leakage flows could contribute significantly to the rotordynamics of a pump, Childs [1] adapted a bulk-flow model (Hirs [18]) to evaluate the rotordynamic forces, Fn and Ft, due to these leakage flows. Though the magnitude and overall form of the model predictions were consistent with the experimental data, Childs' theory yielded some unusual results including peaks in the rotordynamic forces at particular positive whirl ratios, a phenomenon which Childs tentatively described as a "resonance" of the leakage flow. This unexpected phenomenon develops at small positive whirl ratios when the inlet swirl velocity ratio, Γ, exceeds about 0.5. Childs [19] points out that a typical swirl velocity ratio at inlet (pump discharge) would be about 0.5 and may not, therefore, be large enough for the resonance to be manifest. It is clear that a detailed comparison of model predictions with experimental measurement was needed, and it is one of the purposes herein.

LEAKAGE FLOW TEST APPARATUS

A detailed description of the test facility used for the present investigation can be found elsewhere (Chamieh [14], Adkins [15], Jery [17], Arndt [20], Franz[21]), so only a brief description will be given here. The experiments were conducted in water in the Rotor Force Test Facility (RFTF), which was constructed to study fluid induced forces due to imposed whirl motions. The experimental apparatus installed in the RFTF, shown in Figure 2, was designed and constructed to simulate the leakage flow around the shroud from the impeller discharge to the impeller inlet (Zhuang [22], Guinzburg, et al. [23], [24], Guinzburg [25]); the flow is generated by an auxilliary pump. The clearance between the rotating shroud and the stationary casing can be varied by both axial and radial adjustment of the stationary casing. For the present experiment, the initial geometric configuration consists of a straight annular gap inclined at an angle of 45 degrees to the axis of rotation. In order to model losses in the flow, an adjustable face seal was used and was backed off to leave a known clearance (Figure 2). This face seal clearance permittted the pressure drop to be adjusted separately from the flow.

As was mentioned previously, the inlet tangential velocity to the leakage path was shown by Childs [1] to have an effect on the rotordynamic forces. This effect of the inlet swirl was investigated by installing a logarithmic spiral vane in the inlet flow channel (Figure 3). This vane was designed with sufficient solidity to create an isotropic inlet flow. The turning angle was chosen to be two degrees, and this allowed a range of swirl ratios, defined as the ratio of the inlet tangential velocity to the rotor velocity. Thus, as the leakage flowrate and therefore tangential velocity was increased, the swirl ratio could be increased for a fixed rotor speed. Note that the only way to vary the inlet swirl ratio independently of the flow coefficient would be to vary the geometry of the inlet swirl vane. Further discussion on the inlet guide vane and and other

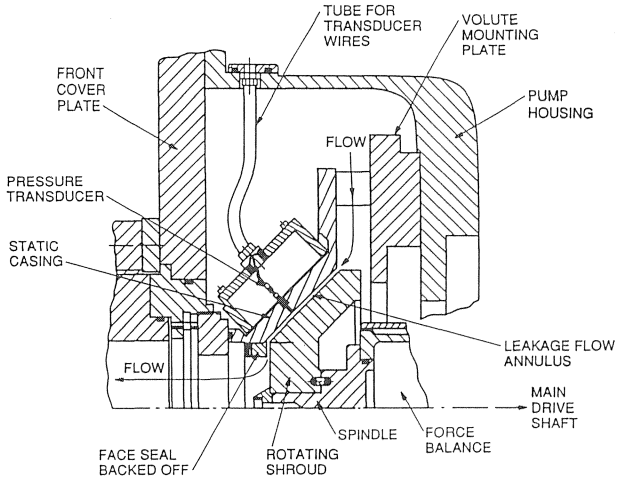

Figure 2. Layout of the Leakage Flow Test Apparatus for Installation in the RFTF.

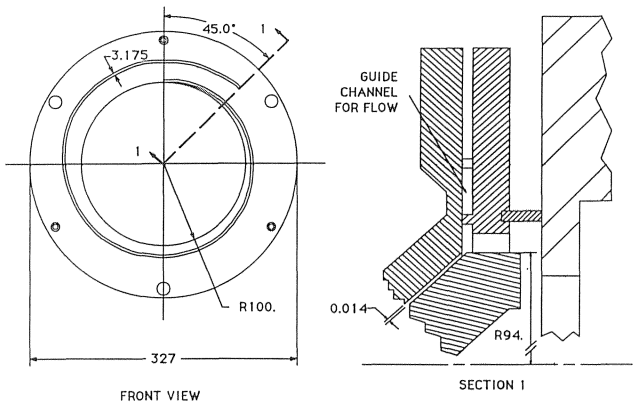

Figure 3. Installation of the Inlet Swirl Vane in the Leakage Flow Test Apparatus.

parts of the experimental equipment can be found in Guinzburg [25].

The experimental investigation of the radial forces and rotordynamic matrices was conducted for a wide range of conditions. The rotordynamic results from the force balance measurements were obtained for different rotating speeds of 500, 1000, 2000 rpm, different leakage flowrates (zero to 3.16×10^{-3} m^3/s), three different clearances, H, and two eccentricities, ε. The range of rotational Reynolds numbers was 462×10^3 to 1851×10^3 and the range of axial flow Reynolds numbers was 2136 to 8546. While the rotational Reynolds numbers for the experimental flows are clearly in the developed turbulent regime, it is possible that the axial flow Reynolds numbers were too slow for the kind of resonances predicited by Childs to occur. The experimental data has been presented previously and the reader is referred to Guinzburg, et al.[26], [23], and Guinzburg, et al. [24], for further detail. The present discussion will be focused on the comparison with the analytical results.

ANALYTICAL MODEL

A numerical simulation of the present experimental conditions was completed using Childs [1] theory. This theory uses a bulk flow model for the leakage flow between the impeller shroud and the pump housing based on the meridional momentum, circumferential momentum, and continuity equations. Any variation in dependent variables across the fluid annulus is neglected. The governing equations are solved by a perturbation expansion which includes only terms which are linear in the eccentricity ratio, ε. The results are sensitive to the inlet conditions, so some details of the boundary conditions are included here.

Description of Loss Coefficients

In the model, losses at the inlet are accounted for by an inlet loss coefficient ξ defined by

$$p(0) = p_s - \frac{1}{2}(1+\xi)(u_s(0))^2 \tag{3}$$

Any reasonable choice of the inlet coefficient seemed to have a negligible effect upon the results of the model and so the value of $\xi = 0.1$ employed by Childs[1] was retained.

At the exit of the leakage path, many pumps have a wear ring seal which provides a flow resistance. This is modelled by the exit loss coefficient C_{de}. When this is used in the mean flow solution, the mass flowrate can be related to the pressure drop across the entire leakage path. Thus, Childs defines the exit loss coefficient in terms of nondimensional variables as:

$$C_{de} = \frac{p(L) - p_e}{\frac{1}{2}(u_s(L))^2} \tag{4}$$

An estimate of the losses for the exit seal can be obtained in the following way. If there are no entrance losses to the seal, and if frictional losses within the seal itself can be ignored, Bernoulli's equation can be applied between the inlet and exit of the seal. If the jet dynamic head is completely lost at the seal exit, this leads to a simple estimate of C_{de}. Using the various shroud clearances, H, and seal clearances, H_s, employed in the experiments we obtain the following wide range of values for C_{de}:

Table 1. Values for C_{de} for different H and H_s.

		H		
		0.140 cm	0.213 cm	0.424 cm
H_s	0.025 cm	47	111	449
	0.050 cm	11	27	109
	0.100 cm	2	6	27

Pressure Distribution

The experiments included pressure distributions measured using three arrays of static pressure taps which were located along meridians on the surface of the stationary casing at equal azimuthal spacings (120 degrees, 240 degrees, 360 degrees). Only a brief summary of these findings will be given here; the reader is referred to Guinzburg [25] for further details. The mean pressures predicted by the model are very sensitive to the selected inlet swirl ratio, Γ, and so it is useful to compare the analytical results for various Γ with the measured pressure distributions (Figure 4). For the higher flowrates, an inlet swirl of $\Gamma = 0$ results in pressures of the same order as those measured experimentally, the implication being that the inlet swirl was effectively zero in the experiments. However, at lower flowrates, the experimental data is better matched, at least near the inlet, by an inlet swirl ratio of $\Gamma = 0.5$. This indicates that the flow rapidly adjusts to a swirl velocity, which is the mean of the rotational velocities of the rotor and the stator. Finally, note that the model and the experiments are substantially in disagreement in terms of the slopes of the pressure

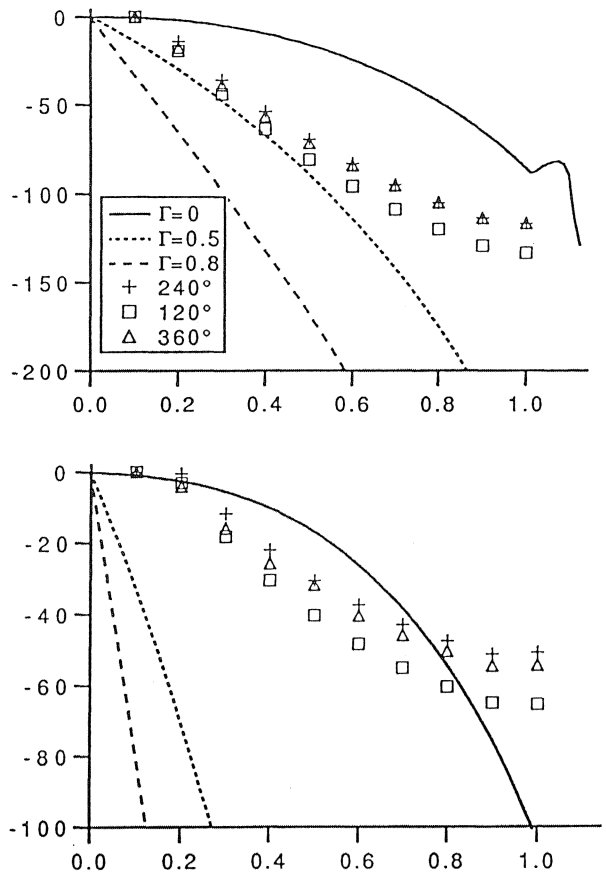

Figure 4. Numerical Predictions of the Pressure Distribution along the Shroud for Different Inlet Swirl Ratios, Compared with the Experimental Observation for 1000 rpm, a Clearance of 0.0424cm, a Flow of 0.632 × 10^{-3} m^3/s (above) and 1.892 × 10^{-3} m^3/s (Bellow).

distributions. The reason for this is not clear at present, but it implies that other predictions of the model may be suspect.

Boundary Conditions

For the solution of the perturbation equations, Childs used the following three boundary conditions which were used in the present calculations:

- The entrance perturbation velocity is zero:

$$\bar{u}_\theta^{\,1}(0) = 0 \tag{5}$$

- The expression for the entrance loss coefficient results in the following relation between $\bar{p}^1(0)$ and $\bar{u}_s^{\,1}(0)$:

$$\bar{p}^1(0) = -(1+\xi)\,\bar{u}_s^{\,1}(0) \tag{6}$$

- The expression for the exit loss coefficient results in the following relation between $\bar{p}^1(1)$ and $\bar{u}_s^{\,1}(1)$:

$$\bar{p}^1(1) = Cde\; u_s^{\,0}(1)\,\bar{u}_s^{\,1}(1) \tag{7}$$

There is no indication that these boundary conditions are physically reasonable assumptions. They all follow from an assumption that the perturbations are essentially quasistatic and can, therefore, be obtained using a linearized perturbation of the steady flow relations. The actual flow perturbation may depart substantially from this quasistatic assumption. There may, for example, be oscillations in the flow before it enters the leakage path. In all cases, the actual losses in the unsteady flow may well be complex and frequency dependent.

Analytical Solution for Turbulent Annular Seals

The validity of the present numerical program was tested by comparing the results to the analytic expressions derived for the dynamic coefficients of annular seals by Childs [27]. In the context of this paper, an annular seal would correspond to a leakage flow in which the rotating shroud was cylindrical and the clearance was constant along its length. The present program produced results similar to those of the typical seal analyzed by Childs [28]. In the seal flow, the results are not sensitive to the perturbation tangential velocity. However, it is expected that the shroud leakage flows will be sensitive to this velocity, as the centrifugal acceleration terms become important in the inclined leakage path.

Exit Flow Models

The exit seal can be analytically modelled in two different ways. First, the seal can be modelled simply by an exit loss coefficient. Then only the inclined portion of the shroud is used in the numerical calculation of the leakage flow. This will be referred to as the partial geometry model. Alternatively, the detailed geometry of the exit seal can be included in the numerical calculation and a residual exit loss coefficient used to model jet mixing losses only. This is referred to as the detailed geometry model.

Estimates of the total exit loss coefficient for the partial geometry model and of the residual loss coefficient for the detailed geometry model were obtained from the experimentally measured flowrates and total leakage pressure drops (Guinzburg [25]). In the H = 0.424 cm and H_s case, this yielded a value of C_{de} = 109 for the total exit loss coefficient in the partial geometry model, a value which is identical with the theoretical estimate given in Table 1. For the detailed geometry model applied to the same case, it was also reassuring to obtain a residual exit loss coefficient close to zero (C_{de} = - 0.2 which is within the uncertainty of the experimental data).

All of the model results presented in the next section utilize the detailed geometry model. Moreover, in order to match the experimental and theoretical pressure gradients as closely as possible, the experimentally measured pressure drops and flowrates were used to calculate a residual exit loss coefficient for each test condition and this loss coefficient was used in the calculation of the rotordynamic forces. It was found, however, that substantial changes in C_{de} had little effect on the rotordynamic results of the model.

COMPARISON WITH EXPERIMENTAL MEASUREMENTS

In this section, the rotordynamic forces which resulted from application of the analysis to the leakage flows of the kind examined experimentally (Guinzburg, et al. [26], [23]) will be presented. It is, however, worthwhile to begin by presenting a typical comparison between the analytical results using the partial geometry model of the exit seal and those using the detailed model. It can be seen in Figure 5 that the rotordynamic forces are substantially different for the two models. This suggests that accurate geometric modelling is essential during implementation of the Childs [1] bulk flow model. Indeed, this geometric accuracy is much more important than the accurate choice of loss coefficients.

The effect of inlet swirl on the rotordynamic forces is next examined. Experimental results included in Figure 6 were obtained with an eccentricity of 0.118 cm, a flow of 0.631 × 10^{-3} m^3/

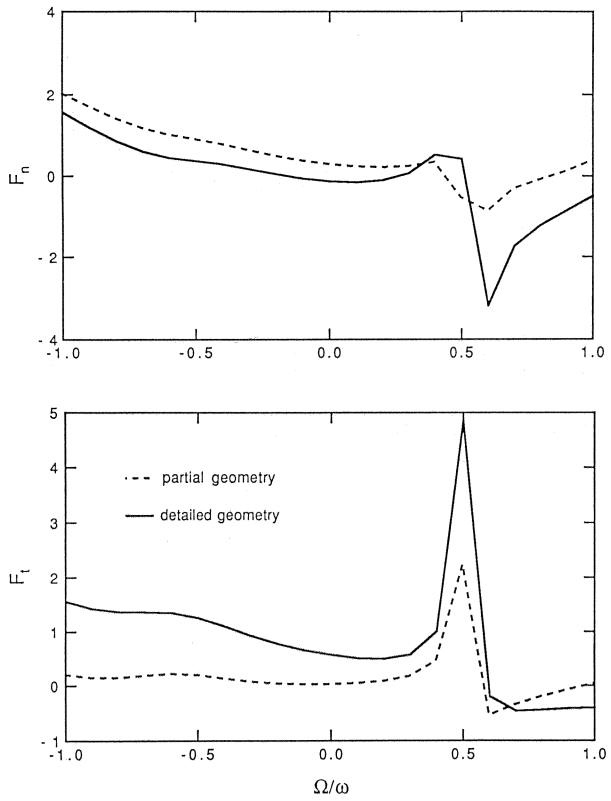

Figure 5. Numerical Predictions of the Normal and Tangential Forces, as a Function of Whirl Ratio for the Following Conditions: inlet swirl, Γ = 0, seal clearance = 0.5 mm, 1000 rpm, 1.264 × 10^{-3} m^3/s, and a clearance, H = 4.24 cm. Results are shown for two analytical models of the exit seal with the same pressure drop. The solid line is obtained with the detailed seal geometry. The dashed line is obtained with the partial geometry and an exit seal loss coefficient.

s (ϕ = 0.078), a speed of 1000 rpm, a clearance of 0.140cm and two values of inlet swirl. The experimental data for both the normal and tangential forces are well behaved and show none of the peaks and troughs present in some of the analytical results (Childs [1]). Analytical results are shown for three values of inlet swirl, including no swirl, and exhibit resonances or peaks when the inlet swirl parameter is different from 0.5. This can be attributed to the fact that the incoming flow is not matched to the flow in the gap region unless Γ = 0.5. Similar results have been obtained for other flowrates (Guinzburg [25]) and it should be noted that the peaks for Γ = 0.5 are particularly pronounced at the smaller flow coefficients. The peaks were found to be particularly pronounced for the cases with no inlet swirl. This may be caused by the fact that the damping of the swirl velocity is reduced at low flowrates. At large positive whirl ratios, the experimental and analytical results are in closest agreement when an inlet swirl ratio of Γ = 0 is used in the model. On the other hand, at whirl ratios close to zero, model values with Γ = 0.5 seem best and at large negative whirl ratios, model values with Γ = 0.8 seem best. These results strongly suggest that there is an additional inlet effect on the swirl velocity that is not properly accounted for in the model.

Though the functional dependence of F_n on the whirl ratio is not necessarily quadratic, nor is F_t linear, it is, nevertheless, of value to the rotordynamicists to fit the data of these curves to the following expressions:

$$F_n = M\left(\frac{\Omega}{\omega}\right)^2 - c\left(\frac{\Omega}{\omega}\right) - K$$
$$F_t = -C\left(\frac{\Omega}{\omega}\right) + k \qquad (8)$$

where M, C, c, K, k are the dimensionless direct added mass (M), direct damping (C), cross-coupled damping (c), direct stiffness (K) and cross-coupled stiffness (k). The cross-coupled mass (m) has been omitted for simplicity, since it is not a significant term. From a stability point of view, the tangential force is most interesting; a positive cross-coupled stiffness is destabilizing, because it drives the forward orbital motion of the rotor. Positive direct damping and negative cross-coupled stiffness are stabilizing because they oppose orbital motion.

A comment on the rotordynamic coefficients is difficult due to the presence of the "resonances." If these were smoothed out, it seems that the model predicts the same direct stiffness as the experiment. However, the normal force obtained from the model results is flatter. Thus, either the mass or cross-coupled damping would be larger for the model than for the experiments. The ratio of the cross-coupled stiffness to direct damping obtained for the model seems to be the same as that obtained from the experiment. However, the cross-coupled stiffness obtained from the model is much larger. It is interesting to note that it increases with swirl (as it does for the experiments).

One of the major parameters influencing the rotordynamic forces is the shroud clearance. Both experimental results (Guinzburg, et al. [26], and Guinzburg [25]) and the present analytical

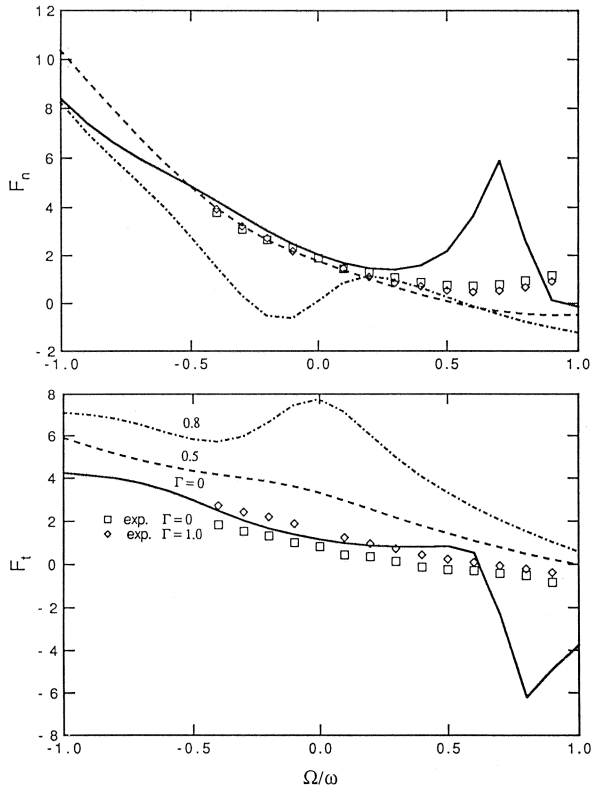

Figure 6. Comparison of the Normal and Tangential Forces, from the Analytical Predictions for Different Inlet Swirl Ratios, Γ = 0, 0.5, and 0.8 with the Experimental Results for the Following Conditions: seal clearance = 0.5 mm, 1000 rpm, a flowrate of 0.632 × 10^{-3} m^3/s, a clearance H = 1.40 cm and an eccentricity ε = 0.118 cm.

results produce rotordynamic forces that are close to being inversely proportional to the shroud clearance.

The effect of the flowrate on the analytical results for an inlet swirl ratio of 0.5 is illustrated in Figures 7 and 8. The experimental results were obtained with an eccentricity of 0.118 cm, a speed of 1000 rpm, a clearance of 0.140cm, and no inlet swirl vane. Figures 7 and 8 are for seal clearances of 0.0025 cm and 0.01 cm, respectively. The normal force obtained analytically exhibits a decrease with flow except in the neighborhood of the peak. This is contrary to the experimental observation that an increase in the flowrate increases the normal force. The effect of the flowrate on the tangential force is also contrary to that of the experimental results. It should be noted, however, that the effect of the flowrate in the experiments was quite small. For inlet swirl ratios different from $\Gamma = 0.5$, the effect of the flowrate on the rotordynamic forces is the same as in the experiments, except near the "resonances" (Guinzburg [25]). Despite this discrepancy between experimental and analytical results on the effect of the leakage flowrate, it is encouraging to note that the magnitudes of the forces are similar.

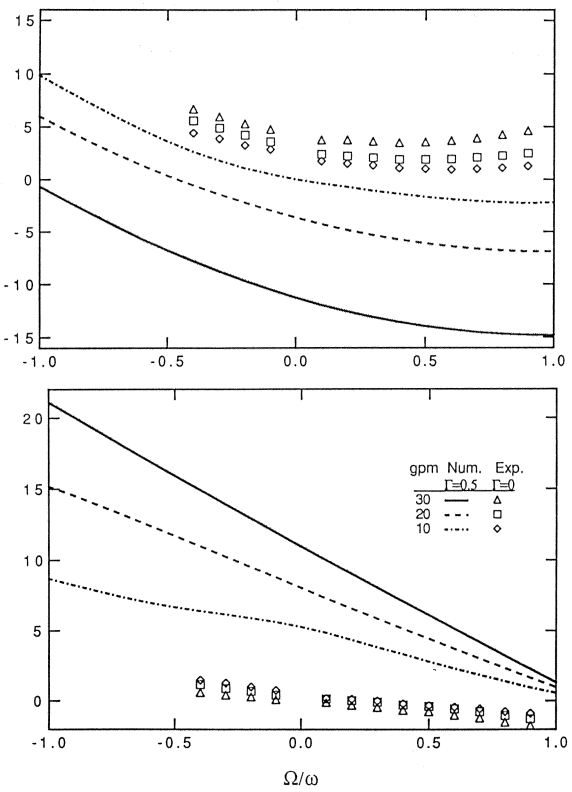

Figure 7. Comparison of the Normal and Tangential Forces, from the Analytical Predictions for an Inlet Swirl Ratio = 0.5 with the Experimental Results for the Following Conditions: different flowrates (0.632×10^{-3} m^3/s, 1.262×10^{-3} m^3/s, 1.892×10^{-3} m^3/s), a seal clearance = 0.25 mm, 1000 rpm, a clearance H = 4.24 cm and an eccentricity ε = 0.0254 cm.

An example of the effect of the seal clearance, H_s, is shown in Figure 9. It can be seen that the tangential force varies inversely with the seal clearance. For positive whirl ratios, the normal force obtained analytically actually decreases with decreasing flowrate. The trends at other flowrates seem inconsistent. However, it would appear that the contribution from the seal portion is significant. It might be expected that as the seal clearance was opened up, the forces would approach those that were obtained with the

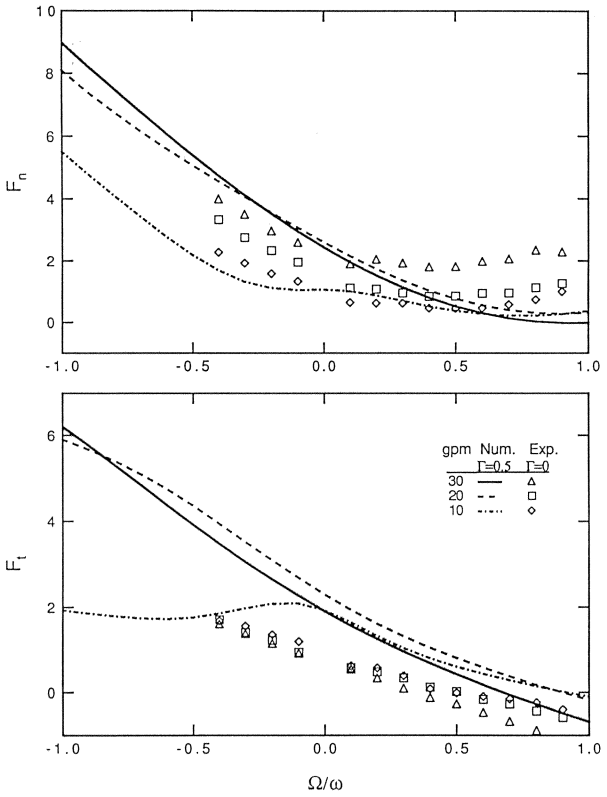

Figure 8. Comparison of the Normal and Tangential Forces, from the Analytical Predictions for an Inlet Swirl Ratio, $\Gamma = 0.5$, with the Experimental Results for the Following Conditions: different flowrates (0.632×10^{-3} m^3/s, 1.262×10^{-3} m^3/s, 1.892×10^{-3} m^3/s), a seal clearance = 1.0 mm, 1000 rpm, a clearance H = 4.24 cm and an eccentricity ε = 0.118 cm.

partial geometry model. Since this was not found to be the case, something is clearly missing from the model. It is suggested that there may be an exit effect on the swirl velocities which is not included in the bulk flow model.

CONCLUSIONS

This study is focused on the fluid-induced rotordynamic forces generated by the discharge-to-suction leakage flows which occur between the shroud and the casing of a centrifugal pump. Specifically, the predicitions of Childs [1] bulk flow model with the experimental measurements of Guinzburg, et al. [29], [26], are compared. The latter utilized a simulated leakage flow with a simple conical geometry and explored the variation in the normal and tangential rotordynamic forces with whirl ratio, eccentricity, clearances, and leakage flowrate. The effect of inlet swirl was also examined by comparing the results with and without an inlet vane that introduced preswirl. Among the observed experimental trends were forces that were inversely proportional to the clearance and a strong function of both the whirl ratio and the leakage flowrate. Moreover, induced preswirl in the same direction as the shroud rotation increased the tangential force and was therefore potentially stabilizing rotordynamically (for more detail see Guinzburg, et al. [26], [23]).

Childs [1] bulk flow model was programmed for the same geometry and used to generate analytical results that could be compared with the experiments. The same boundary conditions based on quasistatic relations for the viscous frictional forces on the rotor and stator were used.

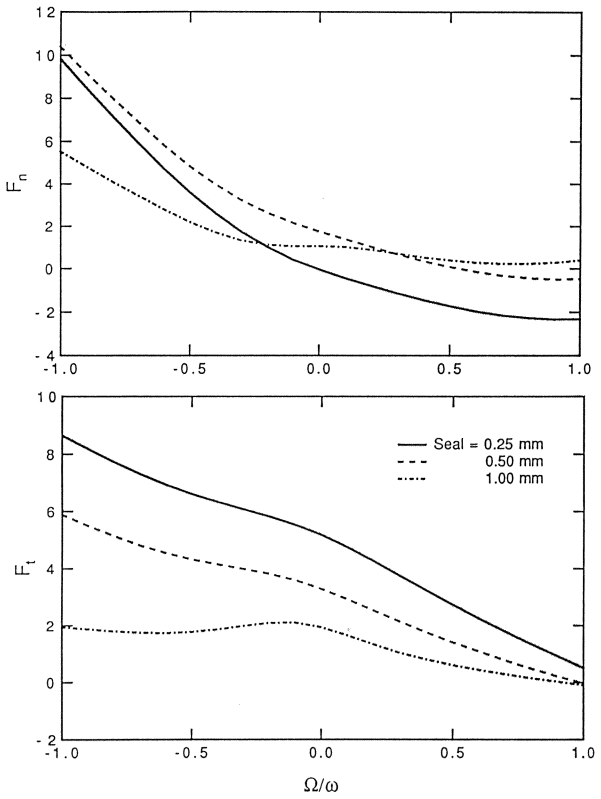

Figure 9. Analytical Predictions of the Normal and Tangential Forces, as a Function of Whirl Ratio for the Following Conditions: Γ= 0.5, 0.632 × 10⁻³ m³/s, 1000 rpm, H = 1.4 cm and three

The comparison with the experiments reveals that the analytical model produces forces, which have the right magnitude and roughly the correct variation with whirl ratio. They also vary inversely with the shroud clearance in a comparable way. However, there are also important discrepancies. Most notably, the experiments exhibited none of the "resonances" which Childs [1] predicited would occur when the inlet swirl ratio exceeded about 0.5. Indeed, further model calculations revealed that the peaks and troughs in the variation of the rotordynamic forces with the whirl ratio (which Childs called resonances) were found to occur whenever the inlet swirl ratio, Γ, was significantly different from 0.5. Thus, they appear when the inlet swirl is not well matched to the mean rotational speed of the flow once the entrance effects have been overcome. The fact that such a phenomenon was not observed in the experiments suggests that other entrance effects (or boundary conditions) on the incoming swirl velocities are not represented in the model. This conclusion seems to be further encouraged by the fact that the tangential forces predicted by the model vary substantially with inlet swirl, whereas those measured experimentally show only a small effect of this variable.

Other discrepancies were also evident. Even at an inlet swirl ratio of 0.5, the variations in the rotordynamic forces with the seal clearance and with flow coefficient are significantly different. Calculation of the rotordynamic coefficients are difficult, because of the "resonances" in the model. Quadratic fits to the F_n and F_t data would, thus, not be very appropriate. All of these suggest the bulk flow model has merit in yielding predictions of the right order; significant improvement is needed in order for it to produce accurate results. Perhaps the boundary conditions need to be altered. Perhaps the quasistatic assumptions used for the perturbation frictional effects and entrance and exit conditions are of limited applicability. Further experiments are clearly needed to provide a firmer foundation for an accurate bulk flow model.

NOMENCLATURE

[A]	rotordynamic matrix normalized by $\rho\pi\omega^2R_2^3L$
C_{de}	exit loss coefficient
F_{ox},F_{oy}	lateral forces on the rotating shroud in the stationary laboratory frame normalized by $\rho\pi\omega^2R_2^3L\varepsilon/R_2$
F_x,F_y	steady hydrodynamic forces normalized by $\rho\pi\omega^2R_2^3L$
$F_n(t)$,$F_t(t)$	unsteady hydrodynamic forces normalized by $\rho\pi\omega^2 R_2^3L\varepsilon/R_2$
H	shroud clearance between rotor and casing
H_s	seal clearance
L	axial length of the shroud
p(s)	pressure in the leakage path
p_e	exit pressure for the leakage flow
p_s	supply pressure for the leakage flow
Q	volume flowrate
R	shroud radius
Re_ω	Reynolds number based on tip speed, $\omega R_2^2/\upsilon$
Re_ϕ	Reynolds number based on meridional velocity, $\frac{2Hu_s}{\nu}$
s	coordinate measured along the meridional in the leakage path, where s = o is the inlet and s = L is the discharge from the leakage path
$u_s(s)$	bulk leakage flow velocity
$u_\phi(s)$	bulk flow tangential velocity
x(t)	instantaneous displacement in the x direction normalized by R_2.
y(t)	instantaneous displacement in the y direction normalized by R_2.
z	axial coordinate
Γ	mean inlet swirl, ratio of inlet fluid tangential velocity to rotor velocity.
ε	eccentricity or radius of the whirl motion.
υ	dynamic viscosity of the fluid
ξ	inlet loss coefficient (typically 0.1)
ρ	density of the fluid
ϕ	flow coefficient, $Q/2\pi R_2^2H\omega$
ω	rotor frequency
Ω	whirl frequency

REFERENCES

1. Childs, D.W., "Fluid Structure Interaction Forces at Pump-Impeller-Shroud Surfaces for Rotordynamic Calculations," ASME Journal of Vibration, Acoustics, Stress, and Reliability in Design, *111*, pp. 216-225 (1989).
2. Frei, A., Guelich, J., Eichorn, G., Eberl, J., and McCloskey, T., "Rotordynamic and Dry Running Behavior of a Full Scale Test Boiler Feed Pump," *Proceedings of the Seventh International Pump Users Symposium*, Turbomachinery Laboratory, Department of Mechanical Engineering, Texas A&M University, College Station, Texas, pp. 81-91 (1990).
3. Pace, S.E., Florjancic, S., and Bolleter, U., "Rotordynamic Developments for High Speed Multistage Pumps," *Proceedings of the Third International Pump Symposium*, Turbomachinery Laboratory, Department of Mechanical Engineering,

Texas A&M University, College Station, Texas, pp. 45-54 (1986).

4. Verhoeven, J., "Rotordynamic Considerations in the Design of High Speed Centrifugal Pumps," *Proceedings of the Fifth International Pump Users Symposium*, Turbomachinery Laboratory, Department of Mechanical Engineering, Texas A&M University, College Station, Texas, pp. 81-92 (1988).
5. Domm, U. and Hergt, P., "Radial Forces on Impeller of Volute Casing Pumps," *Flow Research on Blading*, ed. L.S. Dzung, Netherlands: Elsevier Publishing Co., pp. 305-321 (1970).
6. Hergt, P. and Krieger, P., "Radial Forces in Centrifugal Pumps with Guide Vanes," Proc. of the Inst. of Mech. Eng., *184*, Part 3N, pp. 101-107 (1969-70).
7. Chamieh, D.S., Acosta, A.J., Brennen, C.E., and Caughey, T.K., "Experimental Measurements of Hydrodynamic Radial Forces and Stiffness Matrices for a Centrifugal Pump-Impeller," ASME Journal of Fluids Engineering, *107* (3), pp. 307-315 (1985).
8. Jery, B., Acosta, A.J., Brennen, C.E., and Caughey, T.K., "Forces on Centrifugal Pump Impellers," *Proceedings of the Second International Pump Symposium*, Turbomachinery Laboratory, Department of Mechanical Engineering, Texas A&M University, College Station, Texas (1985).
9. Adkins, D.R. and Brennen, C.E., "Analyses of Hydrodynamic Radial Forces on Centrifugal Pump Impellers," ASME Journal of Fluids Eng., *110* (1), pp. 20-28 (1988).
10. Franz, R., Acosta, A.J., Brennen, C.E., and Caughey, T.K., "The Rotordynamic Forces on a Centrifugal Pump Impeller in the Presence of Cavitation," ASME Journal of Fluids Eng., *112*, pp. 264-271 (1989).
11. Ohashi, H. and Shoji, H., "Lateral Fluid Forces on Whirling Centrifugal Impeller," (2nd Report: Experiment in Vaneless Diffuser), ASME Journal of Fluids Eng., *109*, pp. 100-109 (1987).
12. Bolleter, U., Wyss, A., Welte, I., and Stürchler, R., "Measurements of Hydrodynamic Interaction Matrices of Boiler Feed Pump Impellers," ASME Journal of Vibration, Acoustics, Stress and Reliability in Design, *109*, pp.144-151 (1987).
13. Iversen, H.W., Rolling, R.E., and Carlson, J.J., "Volute Pressure Distribution, Radial Force on the Impeller and Volute Mixing Losses of a Radial Flow Centrifugal Pump," ASME Journal of Eng. for Power, *82* (2), pp. 136-144 (1960).
14. Chamieh, D.S., "Forces on a Whirling Centrifugal Pump-Impeller," Ph.D. Thesis, California Institute of Technology , Pasadena, (1983).
15. Adkins, D.E., "Analyses of Hydrodynamic Forces on Centrifugal Pump Impellers," Ph.D. Thesis, California Institute of Technology (1986).
16. Tsujimoto, Y., Acosta, A.J., and Yoshida, Y., "A Theoretical Study of Fluid Forces on a Centrifugal Impeller Rotating and Whirling in a Vaned Diffuser," Proc. of Adv. Earth-to-Orbit Propulsion Tech. Conf., Hunstville, Alabama (1988).
17. Jery, B., "Experimental Study of Unsteady Hydrodynamic Force Matrices on Whirling Centrifugal Pump Impellers," Ph.D Thesis, California Institute of Technology (1986).
18. Hirs, G.G., "A Bulk-Flow Theory for Turbulence in Lubricant Films," Trans. of the ASME Journal of Lubrication Tech., Paper No. 72-Lub-12, pp. 137-146. (1972).
19. Childs, D.W., "Force and Moment Rotordynamic Coefficients for Pump-Impeller Shroud Surfaces," Proc. of Adv. Earth-to-Orbit Propulsion Techn. Conf., Hunstville, Alabama, NASA Conference Publication 2436, pp. 296-326 (1986).
20. Arndt, N.K.E., "Experimental Investigation of Rotor-Stator Interaction in Diffuser Pumps," Ph.D. Thesis, California Institute of Technology (1988).
21. Franz, R., "Experimental Investigation of the Effect of Cavitation on the Rotordynamic Forces on a Whirling Centrifugal Pump Impeller," Ph.D. Thesis, California Institute of Technology (1989).
22. Zhuang, F., "Experimental Investigation of the Hydrodynamic Forces on the Shroud of a Centrifugal Pump Impeller," Report No. E249.9, Division of Engineering and Application Science, California Institute of Technology (1989).
23. Guinzburg, A., Brennen, C.E., Acosta, A.J., and Caughey, T.K., "The Effect of Swirl on the Rotordynamic Shroud Forces in a Centrifugal Pump," ASME TURBO EXPO, Cologne, Germany (1992).
24. Guinzburg, A., Brennen, C.E., Acosta, A.J., and Caughey, T.K., "The Rotordynamic Characteristics of Leakage Flows in Centrifugal Pumps," ASME Summer Meeting, Los Angeles, California (1992).
25. Guinzburg, A., "Rotordynamic Forces Generated by Discharge-to-Suction Leakage Flows in Centrifugal Pumps," Ph.D. Thesis, California Institute of Technology (1992).
26. Guinzburg, A., Brennen, C.E., Acosta, A.J. and Caughey, T.K., "Measurements of the Rotordynamic Shroud Forces for Centrifugal Pumps," ASME Turbomachinery Forum, Toronto, Canada (June 1990).
27. Childs, D.W., "Finite-Length Solutions for Rotordynamic Coefficients of Turbulent Annular Seals," Transcripts of the ASME, Journal of Lubri. Tech., *105*, pp. 437-445 (1983).
28. Childs, D.W., "Dynamic Analysis of Turbulent Annular Seals Based on Hirs' Lubrication Equation," Transcripts of the ASME, Journal of Lubri. Tech., *105*, pp. 429-436 (1983).
29. Guinzburg, A., Brennen, C.E., Acosta, A.J. and Caughey, T.K., "Rotordynamic Forces Generated by Discharge-to-Suction Leakage Flows in Centrifugal Pumps," Proceedings of Advanced Earth-to-Orbit Propulsion Techniques Conference, Hunstville, Alabama, NASA CP-3092 (1990).

ACKNOWLEDGEMENTS

The authors would like to thank A.J. Acosta and T.K. Caughey for their support and F. Zhuang, A. Bhattacharyya, F. Rahman, and Sandor Nagy for their assistance with the experiments. They would also like to thank NASA George Marshall Space Flight Center for support under Grant NAG8-118.